Catalysis Today 141 (2009) 344–348

Contents lists available at ScienceDirect

Catalysis Today

journal homepage: www.elsevier.com/locate/cattod

Direct synthesis of mesoporous silicalite-1 supported TiO_2–ZrO_2 for the dehydrogenation of EB to styrene with CO_2

Nanzhe Jiang, Dae-Soo Han, Sang-Eon Park *

Laboratory of Nano-Green Catalysis and Nano Center for Fine Chemicals Fusion Technology, Department of Chemistry, Inha University, Incheon, 402-751, Republic of Korea

ARTICLE INFO

Article history:
Available online 16 June 2008

Keywords:
TiO_2–ZrO_2
Mesoporous zeolites
CO_2
Dehydrogenation

ABSTRACT

Direct synthesis route was developed to support TiO_2–ZrO_2 binary metal oxide onto the carbon templated mesoporous silicalite-1 (CS-1). Metal hydroxide modified carbon particles could play a role as hard template and simultaneously support metal components on the mesopores during the crystallization of zeolites. Such supported TiO_2–ZrO_2 binary metal oxides (TZ/CS-1) showed better resistance to deactivation in the oxidative dehydrogenation of ethylbenzene (ODHEB) in the presence of CO_2. These catalysts were found to be active, selective and catalytically stable (10 h of time-on-stream) at 600 °C for the dehydrogenation of ethylbenzene (EB) to styrene (Sty).

1. Introduction

The catalytic performance of nanocomposite metal oxides is strongly influenced by degree and stability of dispersion which control the number of catalytically active sites that are available. To keep high dispersion of active phase, it is necessary to employ supports and make the particles as small as possible [1]. The essential requirements of a better support are nonreactivity with the dispersed phase and high specific surface area. Therefore, selection of a suitable support is an important factor in the design of active catalysts for various reactions. So far, Al_2O_3, SiO_2, ZrO_2 and TiO_2 are the well-established catalyst supports, whereas the development of other supports is still in infancy [2]. The newly discovered mesoporous materials (MCM-41, HMS, SBA-15) with highly ordered pore structures and uniform pore sizes are considered to be promising host materials for nanocrystals, but unfortunately, when compared with those of zeolite materials hydrothermal stabilities are relatively low, especially in the gas phase reaction at high temperature [3].

Recently, a new family of crystalline zeolitic materials was presented by using carbon as hard template. The mesoporous zeolite single crystals could be good candidate as support material with a sufficient number of defect sites throughout the entire zeolite crystal which can efficiently disperse nanocrystals. Positive effects were observed on the performance of mesoporous zeolites in catalysis like better resistance to deactivation [4], significant decrease in transport limitation. Generally, for the supporting metal oxides to the zeolites, impregnation and CVD method are applied. These approaches could be assigned as a post synthesis method. These methods include two steps, one is the preparation of zeolites and another is supporting metal oxide.

The possibility of using ZrO_2 as an acid–base bi-functional catalyst for the oxidative dehydrogenation of EB (ODHEB) with CO_2 has been explored and found that the results were promising, subsequently, Park and co-workers [5] studied ZrO_2 based binary oxide bulk catalysts such as TiO_2–ZrO_2, MnO_2–ZrO_2 and CeO_2–ZrO_2. Also, instead of studying the zirconia based bulk mixed oxide catalysts, supported mixed oxide catalyst system, i.e. CeO_2–ZrO_2/SBA-15 [1] was studied. The influence of SBA-15 support in the ODHEB in the presence of CO_2 was emphasizing for the high activity and selectivity.

Here in, based on our preliminary results, we describe a new method to support TiO_2–ZrO_2 binary metal oxides onto the mesoporous zeolites directly instead of post synthetic methods which need multistep processes for synthesizing support and metal oxides. The surface of carbon nanosphere was modified with metal hydroxides and this modified carbon was utilized as a hard template to synthesize single crystal-shaped mesoporous zeolite. The directly supported metal oxide catalysts TZ/CS-1 showed better resistance to the deactivation in the oxidative dehydrogenation of EB.

2. Experimental

2.1. Synthesis

A simple pH controlled method by using aqueous ammonia was applied to precipitate 0.1 M $TiCl_4$ (Aldrich) and $ZrOCl_2$ (Aldrich)

* Corresponding author. Tel.: +82 32 860 7675; fax: +82 32 872 8670.
E-mail address: separk@inha.ac.kr (S.-E. Park).

0920-5861/$ – see front matter © 2008 Elsevier B.V. All rights reserved.
doi:10.1016/j.cattod.2008.04.033

solution including well-dispersed carbon particles (BP-2000, supplied by M/s. Carbot Corp., USA) under strong mechanical stirring. Metal hydroxide precipitated carbon particles were collected by filtration, washed with H_2O and dried at 100 °C overnight. The modified carbon re-dispersed in the clear sol–gel precursor which was obtained from hydrolysis of TEOS (Aldrich, 98%) with 20% TPAOH (Aldrich) solution. The composition of the resulting synthesis gel was 7 TiO_2: 7 ZrO_2: 100 SiO_2: 20 TPA_2O: 2500 H_2O. The carbon containing zeolite synthesis gel was introduced into a teflon vessel, heated to 165 °C for 1 h. Then, the product was suspended in water, filtered by suction, re-suspended in water, and filtered again. Finally, the product was dried at 100 °C for 10 h, and the organic template and the carbon was removed by controlled combustion in air in a muffle furnace at 550 °C for 10 h.

2.2. Catalytic activity test

The catalytic activity studies were performed in a fixed bed down flow stainless steel reactor (i.d. 10 mm and length 300 mm) under atmospheric pressure. The reactor was loaded with 1.0 g of catalyst sample with the support of quartz wool and conducted the catalyst pretreatment at 600 °C for 2 h in the flow of N_2 (20 mL/min). After the pretreatment of the catalyst, the reaction was conducted at different temperatures either in the flow of N_2 or CO_2. Ethyl benzene was introduced by a peristaltic pump with a feed rate of 9.8 mmol/h. Gaseous and liquid products were analyzed simultaneously by on-line GC (M/s. Younglin Instrument, Acme 6000 series, Korea) equipped with FID. Innowax widebore column (30 m long, 0.32 mm i.d. and 0.25 μm film thickness, supplied by M/s. J&W, USA) was used for the analysis of liquid products comprising of styrene, benzene, toluene and other traces of by-products. Styrene is the main major desired product. Coke was measured directly by weighing the catalysts.

2.3. Characterization

The X-ray diffraction (XRD) patterns were recorded on a Rigaku Multiflex diffractometer (M/s. Rigaku Corporation, Japan) with a monochromated high-intensity Cu Kα radiation (λ = 0.15418 nm, 40 kV, 30 mA). The scanning was within a range of 2θ from 5° to 80° at a rate of 5°/min. Transmission electron microscope (TEM) was carried out on JEM-2010 (M/s. JEOL, Japan) to investigate the morphology and microstructure of samples. N_2 adsorption isotherms were measured at −196 °C using an ASAP2010 gas adsorption analyzer (M/s. Micromeritics Corp., USA). Each sample was degassed at 300 °C for 3 h before the measurement. The total specific surface area was calculated according to the BET equation. Acidity and basicity of the mixed oxide catalysts were investigated by temperature programmed desorption (TPD) of NH_3 and CO_2 respectively, using Chemisorp 2705 unit (M/s. Micromeritics Instrument. Co., USA) equipped with thermal conductivity detector (TCD). Typically, ca. 100 mg of catalyst was pretreated in flowing He at 300 °C for 1 h, cooled to 100 °C and allowed to expose 5% NH_3 (or CO_2) in helium gas mixture with a flow rate of 20 mL/min for 30 min and subsequently the adsorbed NH_3 (or CO_2) was purged with helium at the same temperature for 1 h to remove the physisorbed NH_3 (or CO_2). The chemisorbed NH_3 (or CO_2) was measured in flowing helium with the flow rate of 20 mL/min from 100 °C to 550 °C with the heating rate of 10 °C/min. Raman spectra were obtained on Microscopic Confocal RM2000 Raman Spectrometer (M/s. Renishaw Corp., UK) at room temperature and atmospheric pressure. The exciting wavelength of 325 nm was generated with an Ar^+ laser with a power of 15 mW. The laser beam was focused on the top of the catalyst.

3. Results and discussion

The XRD patterns of pure TiO_2, ZrO_2, binary TiO_2–ZrO_2 oxide and TZ/CS-1 composition were depicted in Fig. 1 (left). Characteristic peaks of crystal phases for ZrO_2 (monoclinic with tetragonal structure) and TiO_2 (anatase and rutile) were observed whereas TiO_2–ZrO_2 binary metal oxide showed only amorphous peak [6]. In the case of TZ/CS-1, no XRD reflections were observed for the supported catalyst in the 2θ range of 5–80° related to TiO_2 or ZrO_2, except typical reflectance for the MFI type zeolite structure of silicalite-1 support. It clearly indicated that no crystalline phase of the mixed oxide was occluded or agglomerated on the surface of silicalite-1 support. On the other hand, none of supported metal oxides shows any segregated pure crystallites detectable by XRD.

According to the IUPAC classification of physisorption isotherms, in Fig. 1 (right), TZ/CS-1 have Type IV isotherms and contain two clear hysteresis loops at relative pressures about $p/p_0 = 0.2$ and at relative pressures higher than $p/p_0 = 0.4$, which is typical for super microporous [7] and mesoporous materials respectively. From the pore size distribution, it is clearly seen that this material has mesopores in the range of 10–80 nm.

SEM image of TZ/CS-1 (Fig. 2(a)) show homogeneous morphology of zeolite crystals with small size impurities. The TEM image of sample (Fig. 2(b)) shows well-developed mesopores inside of zeolite crystals, and small dark areas homogeneously dispersed. Fig. 2(c) and (d) showed the EDXS spectrum of the dark and white area respectively. The Ti, Zr contents were higher in the dark area than the molar composition in the synthesis precursor and on the white area the metal content is much lower than Si. Dark spots sprayed inside of the zeolite crystals could be assigned to the highly dispersed nanosized TiO_2–ZrO_2 binary metal oxides.

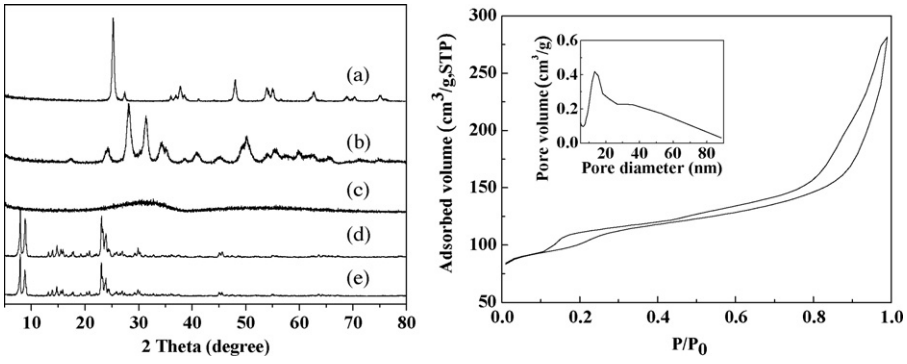

Fig. 1. (Left) XRD patterns of (a) TiO_2, (b) ZrO_2, (c) TiO_2–ZrO_2, (d) CS-1, (e) TZ/CS-1; (right) N_2 full isotherms of TZ/CS-1.

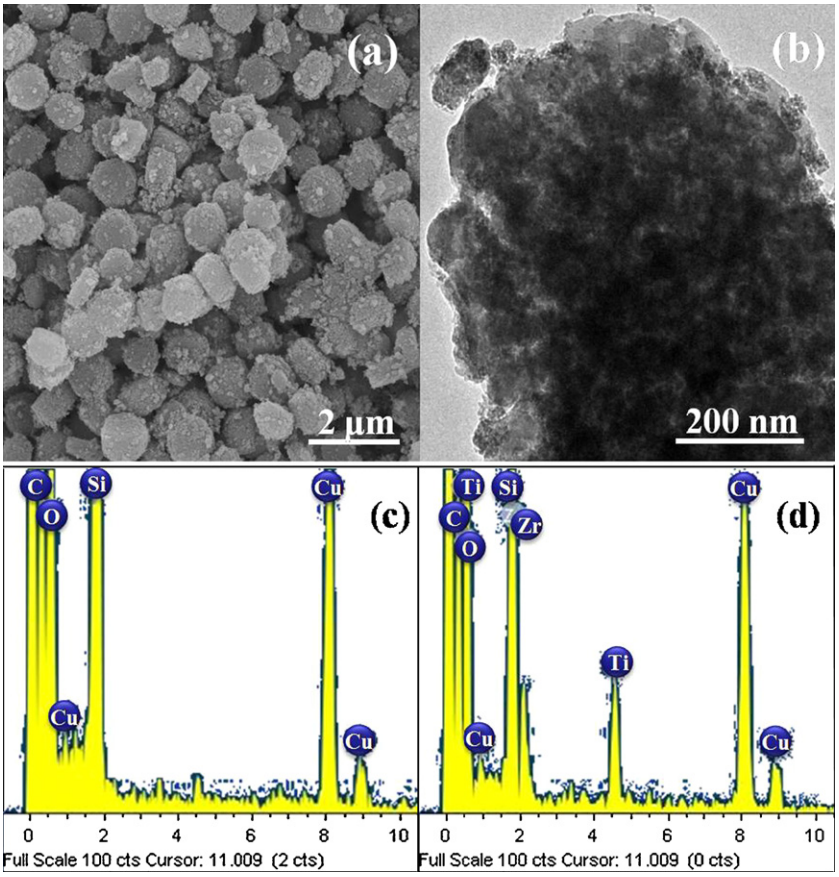

Fig. 2. (a) SEM image, (b) TEM image, (c) EDXS spectrum of the white area in TEM image, (d) EDXS spectrum of the dark area in TEM image of TZ/CS-1 respectively.

The acid strength distributions on the TPD profiles of NH_3 have been analyzed by Berteau and Delmon [8], wherein, the acidic sites were classified as three categories. The amount of NH_3 desorbed below 200 °C is the measure of weak acidic sites, followed by desorption in the temperature range of 200–350 °C which is the measure of medium acidic sites and desorption above 350 °C which is the measure of strong acid sites. In the case of TiO_2–ZrO_2 binary metal oxide the NH_3 TPD peak maximum was at 221 °C, and also it was distributed in a wide range from 150 to 500 °C with high signal intensity (Fig. 3(a), left). This behavior could be explained that the new acidic sites were generated due to mixing of TiO_2 and ZrO_2 and the TiO_2–ZrO_2 mixed oxides not only exhibit higher acidity but also have a large number of acid sites than the pure oxides [9]. For the TZ/CS-1 (Fig. 3(b), left), the NH_3 desorption peak distributed in the range from 150 to 550 °C and desorption at high temperature were more than TiO_2–ZrO_2 bulk oxides which means highly dispersed nanoparticles displayed high proportion of strong acid sites.

The basic strength distribution was investigated using the TPD of CO_2. The TPD profiles of CO_2 for TiO_2–ZrO_2 binary metal oxide and the TZ/CS-1 were shown in Fig. 3 (right). It has been demonstrated that the strength and number of basic sites of TiO_2–ZrO_2 mixed oxide were much higher than that of its individual oxides (TiO_2 and ZrO_2) [6]. The temperature maxima for TiO_2–ZrO_2 (Fig. 3(a), right) and TZ/CS-1 (Fig. 3(b), right) are 221 and 216 °C respectively for the weak basic sites. The TPD profile of TZ/CS-1 possessed two more peaks with the maxima at 404 and 504 °C. It clearly indicates that strong basic sites were generated

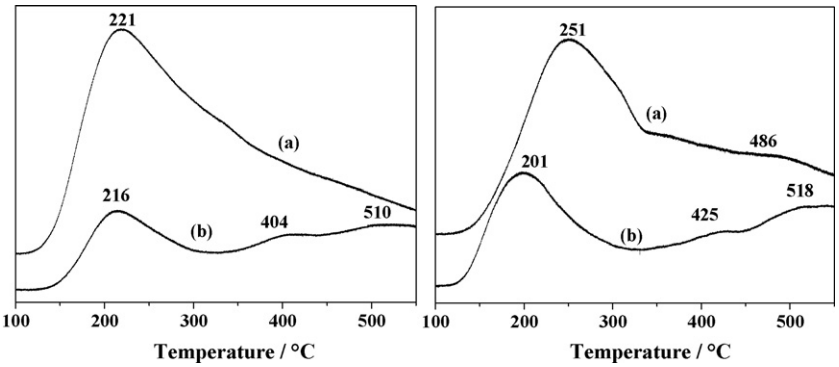

Fig. 3. (Left) TPD profiles of NH_3, (a) TiO_2–ZrO_2 binary metal oxide, (b) TZ/CS-1; (right) TPD profiles of CO_2, (a) TiO_2–ZrO_2 binary oxide, (b) TZ/CS-1.

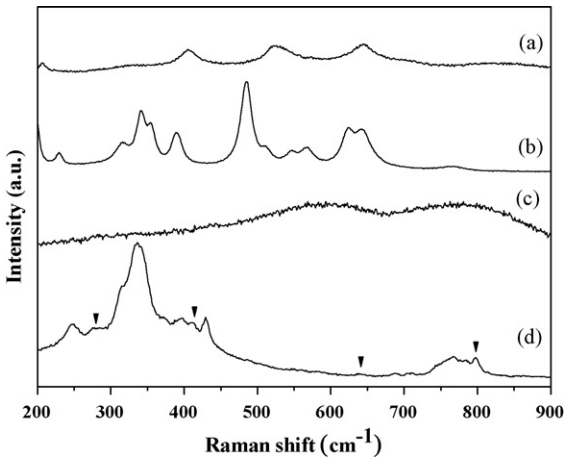

Fig. 4. Raman spectra of (a) TiO_2, (b) ZrO_2, (c) TiO_2–ZrO_2, (d) TZ/CS-1.

more in the present preparation. Basic site distribution from weak to strong is different for supported and unsupported TiO_2–ZrO_2 binary metal oxides. The strong basic sites are in relatively high proportion for the supported TiO_2–ZrO_2 in the TZ/CS-1.

The FT-Raman spectra of various samples are presented in Fig. 4. The Raman spectrum of TiO_2 anatase exhibits bands at 144, 199, 399, 520, 638 cm^{-1} and the TiO_2 rutile at 144 and 611 cm^{-1}, respectively [10]. And the Raman spectra of monoclinic and tetragonal ZrO_2 exhibits bands at 103, 181, 190, 222, 310, 337, 382, 474, 499, 540, 559, 620, 636, 763 cm^{-1} and a shoulder at 261–270 cm^{-1}, respectively [11]. The spectrum of TZ/CS-1 contains broad bands at around 280, 412, 640 and 800 cm^{-1} which should be characteristic for a $ZrTiO_4$ compound [12], while the TiO_2–ZrO_2 sample did not give clear information of any crystal structures which were mentioned above. Fung and Wang [13] have reported that the TiO_2–ZrO_2 was amorphous when it was calcined at temperatures less than 600 °C. But in the case of direct supported TiO_2–ZrO_2, we obtained the solid solution for TiO_2–ZrO_2, it may due to nature of the highly dispersed binary metal oxides on the carbon template.

Park and co-workers [6] studied catalytic activity of individual oxides and TiO_2–ZrO_2 oxides in the dehydrogenation of EB to styrene. The catalytic activity of TiO_2–ZrO_2 catalyst was almost doubled than those of individual oxides and also concluded that the TiO_2–ZrO_2 catalysts are suitable for the CO_2 coupled process. The formation of amorphous TiO_2–ZrO_2 mixed oxide, enhancement in surface areas, and the hike in acidic and basic sites number and strength might be the reasons for the higher catalytic activity of these mixed oxides towards conversion of EB and styrene selectivity than those of their individual oxides. Over zirconia based binary metal oxides, the dehydrogenation of EB to styrene followed the acid–base bi-functional mechanism [14].

The catalytic activity of mesoporous silicalite-1 supported TiO_2–ZrO_2 binary metal oxides was tested for the ODHEB to styrene in the presence of CO_2 and N_2 (Fig. 5, left). In the presence of CO_2, the reaction showed higher conversion of EB and selectivity to styrene. The role of CO_2 has clearly been explained recently in the ODHEB over redox [15] and acid–base catalysts. In the presence of CO_2, supported TiO_2–ZrO_2 binary metal oxides showed the same result with bulk TiO_2–ZrO_2 binary metal oxides and following the acid–base mechanism. TZ/CS-1 showed maximum selectivity of styrene 92% and this was relatively low compared to that on bulk oxides 98% (from ref. [6]). Decreased selectivity may due to the presence of more strong acid and basic sites which could cause the cracking of EB.

In the previous work, the stable activity of TiO_2–ZrO_2 mixed oxide catalysts was observed in the dehydrogenation of EB to styrene even at elevated temperatures in the presence of CO_2 [6]. Such phenomena was also observed for the Fe_2O_3/Al_2O_3 catalyst during the dehydrogenation in the presence of CO_2 and concluded that the CO_2 suppressed the deactivation of the catalyst during the dehydrogenation of EB [15]. In both the cases, the coke deposition on the surface of the catalyst was lower in the presence of CO_2 than that of its absence and this was believed as main reason for the deactivation of catalysts [6]. The coke deposition on the mesoporous silicalite-1 supported TiO_2–ZrO_2 were compared to that one on pure TiO_2, ZrO_2 and TiO_2–ZrO_2 bulk oxides (Fig. 5, right). The amount of coke deposition was the smallest for the TZ/CS-1. Well-developed mesopores in the zeolites will shorten the diffusion pathway but also disperse supported catalysts to the nanometric levels. The deposited coke on such highly dispersed nanosized binary TiO_2–ZrO_2 oxides (Fig. 2b) will be active and easy to remove. The catalytic activity of TZ/CS-1 was stable even at higher temperature at 650 °C or in the presence of N_2 (Fig. 5, left). It could be assigned to the less coke deposition on the TiO_2–ZrO_2 binary oxides which was supported on the carbon templated mesoporous silicalite-1.

4. Conclusion

TiO_2–ZrO_2 binary oxides directly supported through the carbon templating method. Those metal oxides are highly dispersed inside of the silicalite-1 crystals with nanorange particle size. Such supported TiO_2–ZrO_2 binary oxides showed higher proportion of strong acid–base sites in the TPD analysis which might be due to the formation solid solutions ($ZrTiO_4$). In the ODHEB to styrene, through the time-on-stream, catalytic activity of TZ/CS-1 catalyst was stable which is caused by less coke deposition. Mesoporous

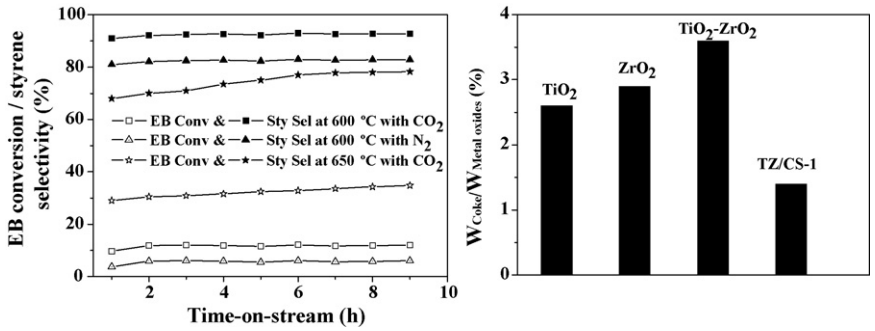

Fig. 5. (Left) Catalytic activity on TZ/CS-1 catalyst in the presence and absence of the CO_2, reaction conditions: P = 1 atm, W/F = 16.73 g cat, h/mole, CO_2/EB = N_2/EB = 5.1 (molar ratio); (right) comparison of coke contents per unit mass of catalysts, wt.% (data for TiO_2, ZrO_2, and TiO_2–ZrO_2 from reference [6]), reaction conditions: in the presence of CO_2, temperature 600 °C, time 10 h, P = 1 atm, W/F = 16.73 g cat, h/mole, CO_2/EB = 5.1 (molar ratio).

silicalite-1 material is one of the promising supports for the development of highly stable metal oxide catalyst.

Acknowledgements

This work was supported by the KOSEF for A3, NRL (36379-1), BK21 projects and MOCIE for Nano Center for Fine Chemicals Fusion Technology.

References

[1] D.R. Burri, K.-M. Choi, J.-H. Lee, D.-S. Han, S.-E. Park, Catal. Commun. 8 (2007) 43.
[2] B.M. Reddy, P. Lakshmanan, P. Bharali, P. Saikia, G. Thrimurthulu, M. Muhler, W. Grunert, J. Phys. Chem. C 111 (2007) 10478.
[3] F.-S. Xiao, Y. Han, Y. Yu, X. Meng, M. Yang, S. Wu, J. Am. Chem. Soc. 124 (2002) 888.
[4] C.H. Christensen, I. Schmidt, A. Carlsson, K. Johannsen, K. Herbst, J. Am. Chem. Soc. 127 (2005) 8098.
[5] B.M. Reddy, D.-S. Han, N. Jiang, S.-E. Park, Catal. Surv. Asia 12 (2008) 56.
[6] D.R. Burri, K.-M. Choi, S.-C. Han, A. Burri, S.-E. Park, Bull. Korean Chem. Soc. 28 (2007) 53.
[7] Z. Yang, Y. Xia, R. Mokaya, Adv. Mater. 17 (2005) 2789.
[8] P. Berteau, B. Delmon, Catal. Today 5 (1989) 121.
[9] H. Zou, Y.S. Li, Appl. Catal. 265 (2004) 35.
[10] I.R. Beattie, T.R. Gilson, J. Chem. Soc. A (1969) 2322.
[11] J. Miciukiewicz, T. Mang, H. Knözinger, Appl. Catal. A: Gen. 122 (1995) 151.
[12] B.M. Reddya, P.M. Sreekanth, Y. Yamadab, Q. Xu, T. Kobayashi, Appl. Catal. A: Gen. 228 (2002) 269.
[13] J. Fung, I. Wang, J. Catal. 130 (1991) 577.
[14] B.M. Reddy, A. Khan, Catal. Rev. 47 (2005) 257.
[15] N. Mimura, M. Saito, Catal. Lett. 58 (1999) 59.